ELSEVIER

Catalysis Today 70 (2001) 393–409

CATALYSIS TODAY

www.elsevier.com/locate/cattod

Evolution of spatiotemporal temperature patterns in monolithic catalytic reactor

Robert Jahn [a], Dalimil Šnita [a], Milan Kubíček [b], Miloš Marek [a,*]

[a] *Department of Chemical Engineering, Center for Nonlinear Dynamics of Chemical and Biological Systems, Prague Institute of Chemical Technology, 166 28 Prague 6, Czech Republic*

[b] *Department of Mathematics, Center for Nonlinear Dynamics of Chemical and Biological Systems, Prague Institute of Chemical Technology, 166 28 Prague 6, Czech Republic*

Abstract

Experimental data on dynamic evolution of spatiotemporal temperature patterns and temporal conversion patterns for CO and hydrocarbon oxidation and NO reduction in a monolithic catalytic reactor reflecting variations of inlet conditions are presented. Possibility of increasing conversion of NO_x reduction by periodic variation of inlet conditions is experimentally documented.

Keywords: NO_x reduction; Dynamical measurement; Catalyst; Monolith; Spatiotemporal temperature patterns; Non-stationary operation

1. Introduction

Monolithic catalytic reactors are widely used as automobile catalytic converters [1] and thus represent the by far most common catalytic reactor. Monolithic reactors are most often operated under non-stationary conditions as inlet conditions vary in dependence on driving conditions. Simultaneous oxidation of CO and hydrocarbons and reduction of NO_x under stoichiometric conditions have been solved by the introduction of three-way catalysts. Combustion under lean conditions (an excess of oxygen) can keep engine efficiency higher. However, catalytic reduction of nitrogen oxides in the presence of oxygen is difficult. Recently, controlled periodic variation of inlet conditions between lean (excess of oxygen) and rich (excess of reducing components) has been proposed and used for NO_x control by selective catalytic reduction [2–6]. Storage of nitrogen oxides on catalytic surface in lean period and its reduction in the rich period is used for enhancing the overall conversion of nitrogen oxides. Most catalysts for NO_x reduction operate within a specific temperature window. Hence the control of temperature within the monolith is important to achieve maximum possible conversions.

Evolution of temperature patterns in monolithic catalytic reactors has been followed experimentally by several authors [7–9]. However, until now, no detailed experiments on spatiotemporal temperature patterns in the course of the "light-off" of the monolithic reactor and/or in the course of periodic variation of inlet conditions were presented in the open literature. In the following, we present such a data and discuss the evolution of spatiotemporal temperature patterns.

2. Experimental equipment

The experimental set-up used for experiments is depicted in Fig. 1. Two different types of experimental reactors were used. The first one enabled the

* Corresponding author.

0920-5861/01/$ – see front matter
PII: S0920-5861(01)00346-7

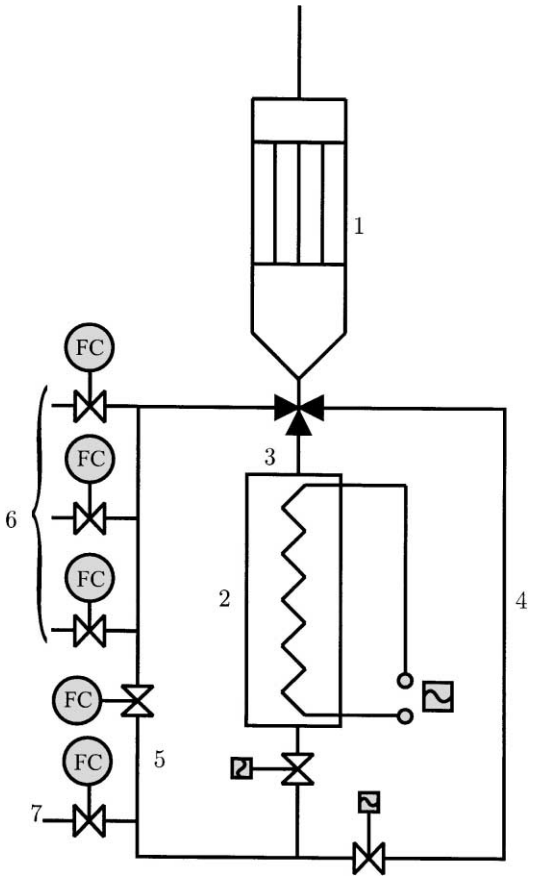

Fig. 1. Scheme of experimental reactor set-up: (1) reactor; (2) electrical heater; (3) hot air stream; (4) cooling air stream; (5) bypass for admixing (for fast response); (6) inlet mass-flow controllers (FC); (7) air mass-flow controller.

measurement of spatially 2D spatiotemporal temperature patterns [10] and the second one was used for logging of axial temperature patterns during fast periodic variations of inlet conditions. The reactor has been equipped for measurements of spatially 2D temperature pattern with shifting mechanism that enabled positioning of thermocouples within the channels of the reactor. The timing of the positioning and the entire process of data acquisition was controlled by industrial PC. Temperature profiles inside the monolithic reactor were measured by thin thermocouples (diameter 0.25 mm) inserted from the outlet face of the monolith (cf. the location of thermocouples depicted in Fig. 2).

The inlet composition and flow rate were controlled by mass-flow controllers (Bronk-horst F-203, F-201), admixture gases were obtained from gas pressure vessels and air from an oil-less compressor. The periodic variation of inlet composition (switching between the reacting and the cooling stream) was managed by two solenoid valves that controlled bypass of electrical heater in the cooling half-period, cf. Fig. 1. Inlet flow temperature was controlled by PID temperature controller based on temperature value from the thermocouple inserted in front of the monolith. The inlet and outlet stream compositions were monitored (after cooling and filtering) by an analytical system consisting of infra-red analyzers (NO/NO_x and CO/CO_2; ABB (HARTMAN & BRAUN), URAS 14, Advanced Optima) and of paramagnetic analyzer (oxygen; ABB (HARTMAN & BRAUN), Magnos 16, Advanced Optima). For NO_x analysis, the NO_2 to NO chemical converter was used. Measurements of 2D spatiotemporal patterns were performed by two methods — dynamic and stationary. The dynamic method used continuous shifting of thermocouples within the reactor, cf. Fig. 2 and supplied data on the evolution of axial spatiotemporal temperature patterns in individual channels (18 channels from the total of 1122 were used for measurement). Single "snapshot" of temperature pattern in the entire monolith could be obtained within 22 s.

The stationary method consisted of periodically repeated sampling of temperatures at chosen axial positions. Comparison of spatiotemporal patterns measured by the two methods enabled the estimation of the reproducibility of measurements. The monoliths used in experiments were of standard type (cell density 400 CPI) available from different industrial producers. Three different monoliths were used: Pt/Rh (5:1)/Al_2O_3, Pt (1 wt.%) on Al_2O_3 on ceramic support and Pt (1 wt.%) on Al_2O_3 on metallic support.

3. Experimental results

3.1. Spatiotemporal temperature patterns — "light-off" in CO combustion

Conversion efficiency of monolith catalysts used in mobile applications can be increased by accelerating the "light-off". The study of the evolution of spatiotemporal temperature patterns in the course of

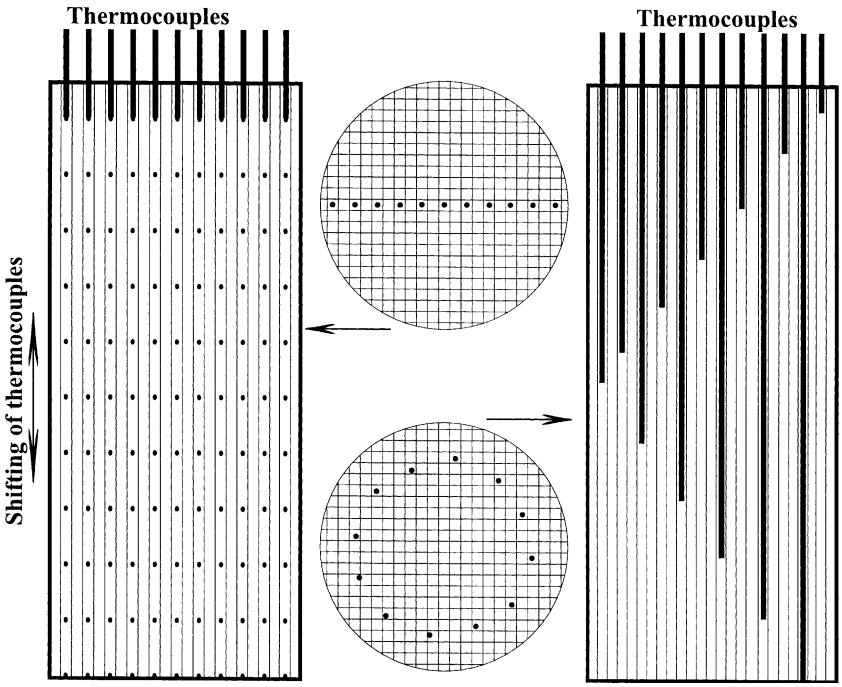

Fig. 2. Two ways of measurement of spatiotemporal temperature patterns in the monoliths — schematically. Left: measurement of spatially 2D temperature patterns by shifting thermocouples ● ● ● ● ● — axial location of 11 measurement positions. Used for dynamic and stationary measurements, namely for measurements under radially nonuniform inlet flow velocity distribution, cf. explanation in the text. Right: measurement of axial (1D) temperature patterns by thermocouples located at fixed positions. Used for measurements under uniform inlet flow velocity distribution and in periodic operations.

the "light-off" can be used in the improvement of "light-off" characteristics. In axial flow catalysts used in cars, flow velocities and temperatures in the central layers of the monolith are higher than in the outer layers. The flow velocity can be 50% higher in the control area covering one-third of the cross-section [11,12]. Authors [13] considered on the basis of actual measured data that velocity in the center at the inlet of the monolith can be more than four times higher than average flow velocity. Poisoning and thermal deterioration of the catalyst is then stronger in the center than in the outer layers. This is one of the reasons why the catalyst actually used in cars is designed with an excess capacity. The actual distribution of flow velocities and the actual spatiotemporal pattern of the activity of the catalyst then determine the evolution of spatiotemporal temperature patterns and the process of "light-off".

Oxidation of CO by air has been used to study the evolution of spatiotemporal temperature patterns and ignition ("light-off") close to the catalyst ignition point and to investigate the effects of radially nonuniform inlet flow distribution. The monolithic reactor under these conditions exhibited hysteresis in dependence of the outlet concentration on inlet temperature, i.e., multiple steady states could be observed in the extinction–ignition region.

Experiments on the "light-off" behavior of the monolithic reactor were carried out for different inlet temperatures and radial flow velocity patterns (uniform and parabolic-like). The used ceramic monolithic reactor contained catalyst Pt/Rh on Al_2O_3 with channel density 400 CPI, the monolith had diameter 48 mm and length 120 mm. The experimental procedure was as follows: First, constant temperature air flow passed through the reactor. After the stabilized initial temperature profile was recorded, the composition of the inlet stream was changed by adding reacting species, e.g., carbon monoxide (1 vol.%),

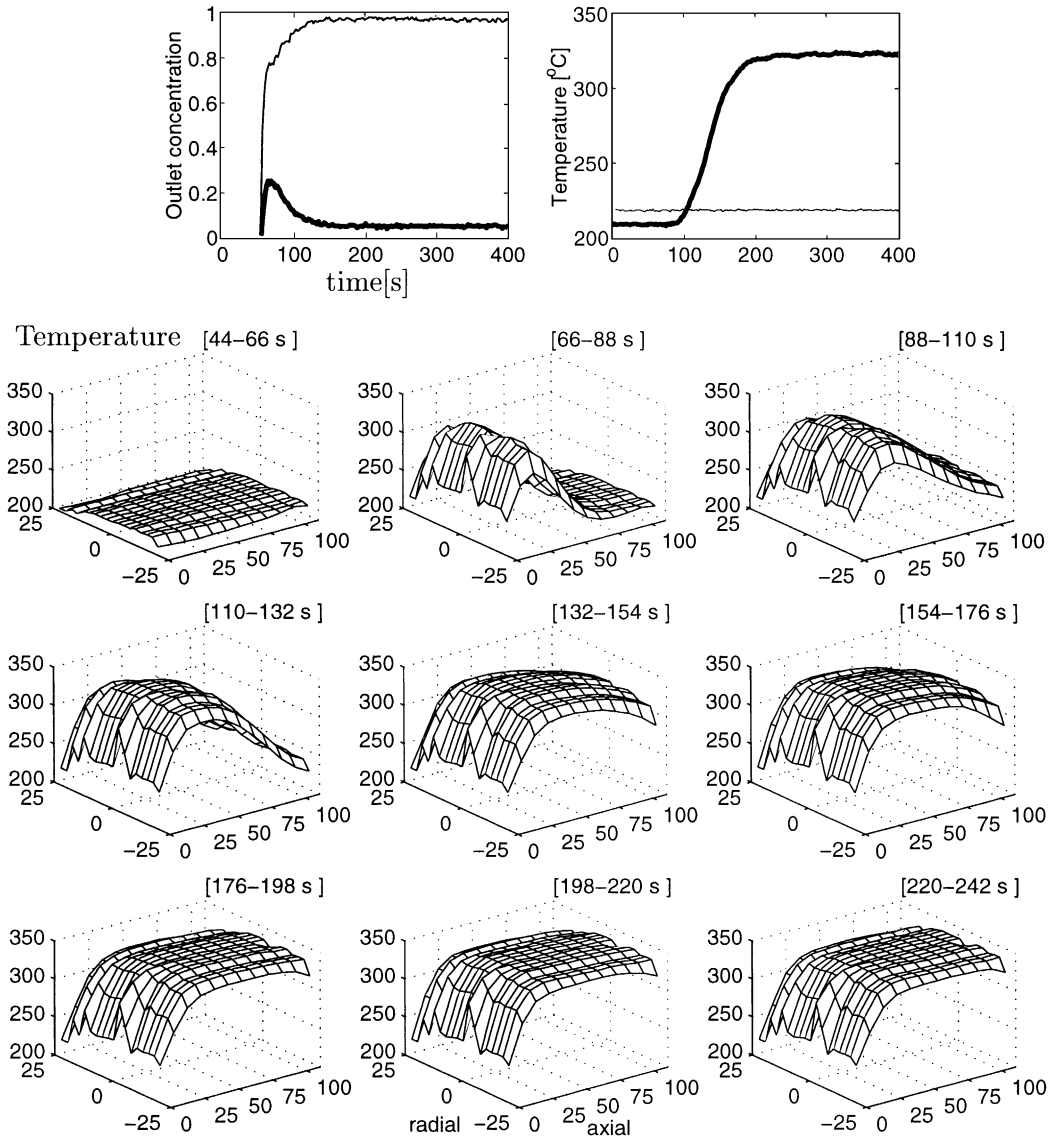

Fig. 3. Evolution of spatiotemporal temperature patterns in monolithic reactor (bottom), radial and axial coordinates in mm, temperature in °C, $T_{in} = 220°C$, $V_{in} = 75$ l/min, *uniform* inlet flow distribution, fully ignited reactor; (top) course of outlet concentrations in vol.% (CO — thick line, CO_2 — thin line), temperature-inlet (thin line) and outlet (thick line).

while the temperature scanning inside the monolithic structure was continued (dynamic method). The outlet concentrations were also recorded. The data were saved on the PC for further processing. The experiment was terminated when the outlet concentration and the inside temperature profiles were stabilized. The results of such experiments are depicted in Figs. 3–5 and discussed below. Experimental conditions are summarized in Table 1.

3.1.1. Uniform inlet flow velocity distribution

The results of the "light-off" experiment for radially uniform inlet flow pattern are depicted in Fig. 3. The reaction front is ignited in the front part of the reactor

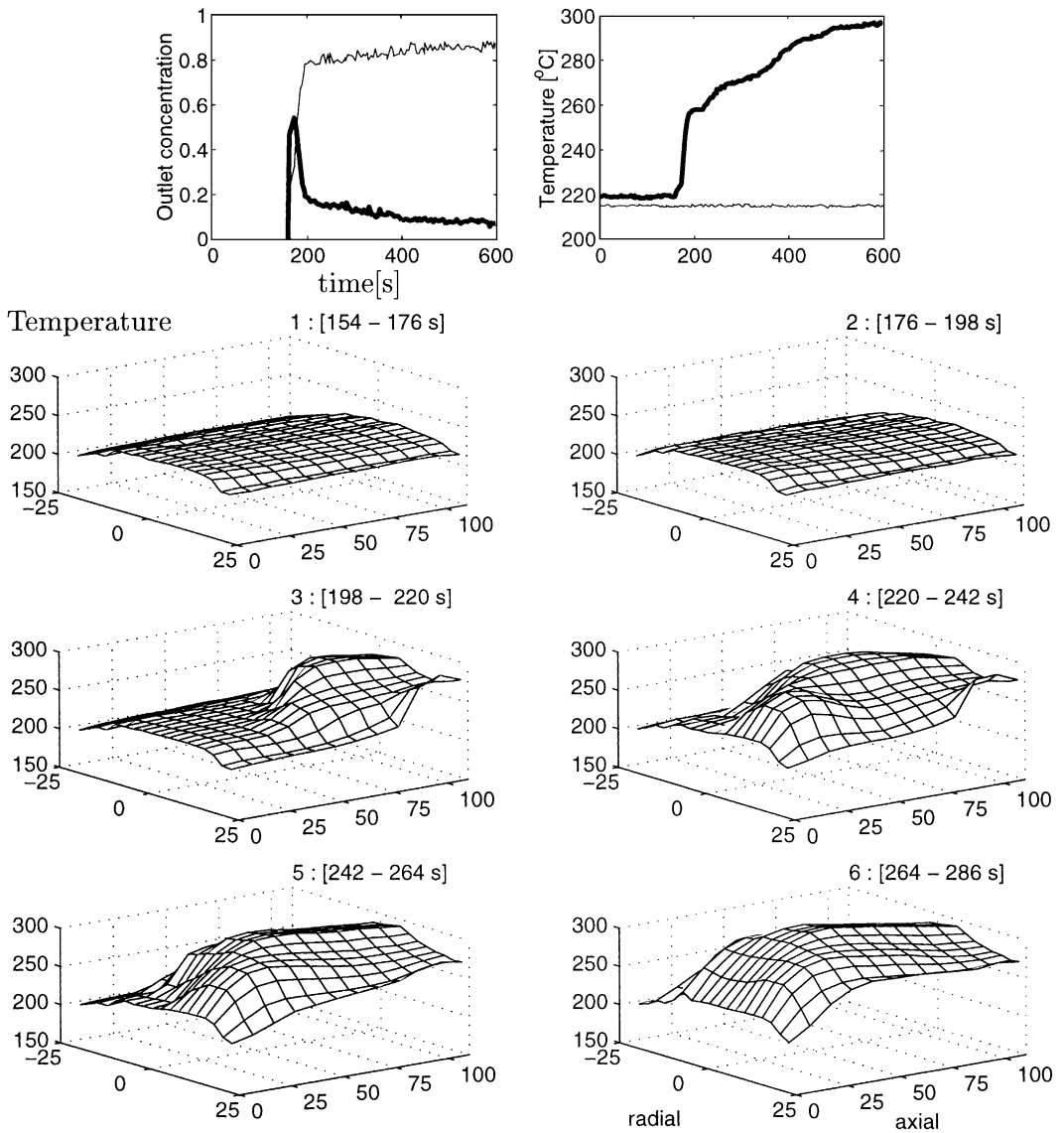

Fig. 4. Evolution of spatiotemporal temperature patterns in monolithic reactor (bottom), radial and axial coordinates in mm, temperature in °C, $T_{in} = 215$°C, $V_{in} = 75$l/min, *nonuniform* inlet flow distribution with maximum in the center, fully ignited reactor; (top) course of outlet concentrations in vol.% (CO — thick line, CO_2 — thin line), temperature-inlet (thin line) and outlet (thick line).

Table 1
Experimental conditions for "light-off" experiments

figure*	T_{in} (°C)	V_{in} (l/min)	c(CO) (vol.%)	$c(C_3H_6)$ (vppm)	c(NO) (vppm)	Inlet flow distribution
3	220	75	1	–	–	Uniform
4	215	75	1	–	–	Nonuniform
5	250	75	1	–	–	Nonuniform

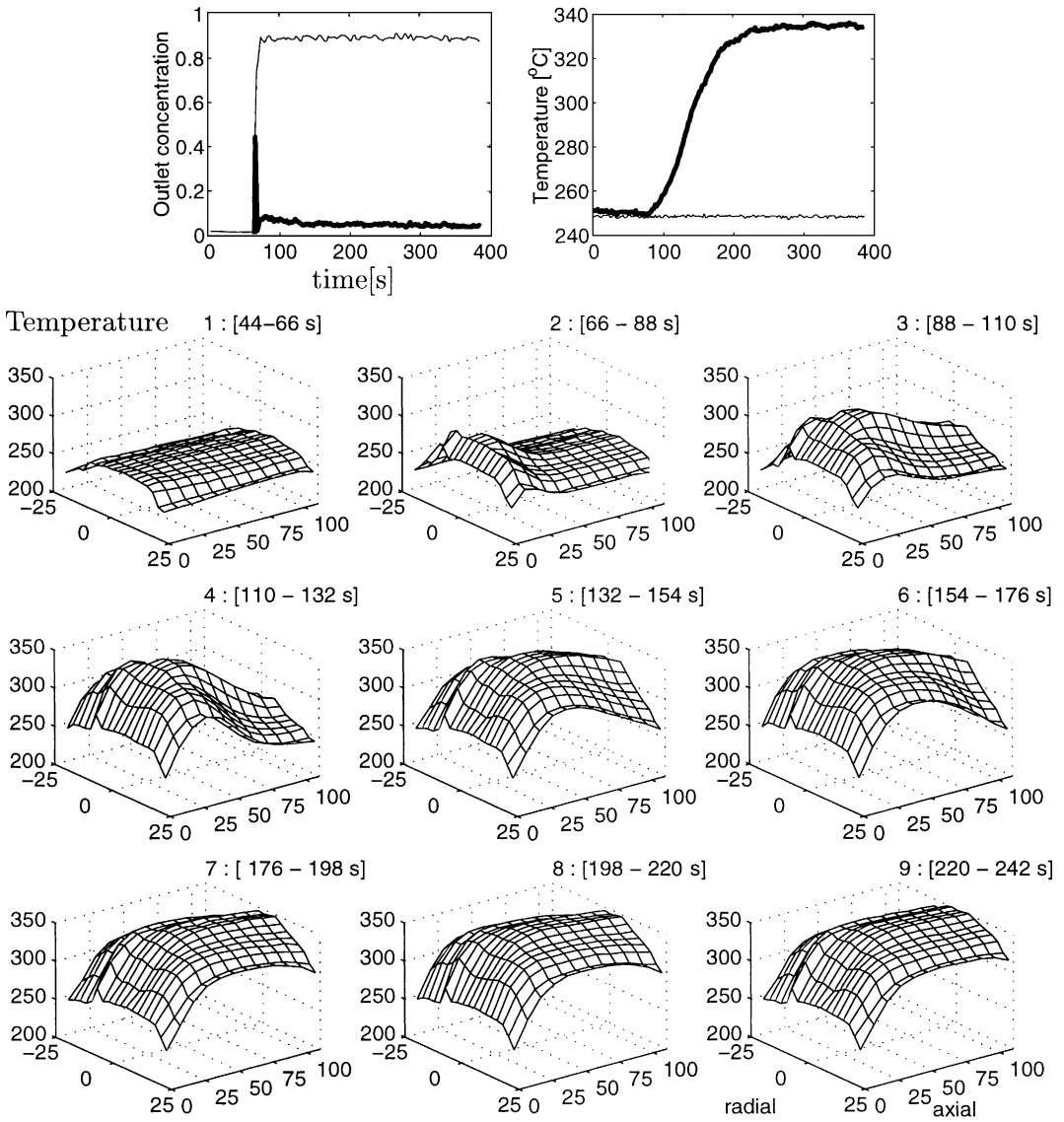

Fig. 5. Evolution of spatiotemporal temperature patterns in monolithic reactor (bottom), radial and axial coordinates in mm, temperature in °C, $T_{in} = 250°C$, $V_{in} = 75\,l/min$, *nonuniform* inlet flow distribution, fully ignited reactor; (top) course of outlet concentrations in vol.% (CO — thick line, CO_2 — thin line), temperature-inlet (thin line) and outlet (thick line).

over the entire reactor cross-section and temperature maxima are located at the same axial distance from the reactor inlet. The monolith is heated up by the reaction heat which is accumulated in the monolithic structure until the relatively constant temperature along the reactor is achieved. Only low radial temperature gradients are present in the outer boundary area resulting from a nonadiabatic operation of the monolithic reactor. Different course of the "light-off" was observed in the case of lower inlet temperature close to ignition temperature. The ignition then occurs in the rear part of the reactor. Temperature maximum is propagated to the front part until it is stabilized near the monolith center.

3.1.2. Effects of nonuniform inlet flow velocity distribution

The nonuniform inlet flow velocity distribution was realized by inserting metallic mesh at the face of the monolith which controlled the flow distribution. In the case of the increased flow rate in the central part of the monolith metallic mesh with central hole (diameter 10 mm) has been used, cf. Fig. 13 (top). Spatiotemporal temperature patterns depicted in Fig. 4 for inlet temperature 215°C illustrate the formation of hot spot in the reactor rear part and its propagation to the inlet of the reactor where it is stabilized. We can observe that the ignition front is radially nonuniform and propagation takes place also nonuniformly (compare with the radially uniform ignition for the uniform inlet flow rate in Fig. 3). After the stabilization of the hot spot in the front part of the reactor, the radial temperature profile becomes flat and the outlet concentration of CO is near zero. The ignition in the front part of the reactor for higher inlet temperature (250°C) is shown in Fig. 5. The nonuniform inlet flow distribution induces local temperature maximum at the center of the middle part of the monolithic reactor.

Comparison of evolution of spatiotemporal temperature patterns for uniform and nonuniform inlet flow velocity distribution shows that differences in pattern evolution are observed mainly during the ignition before the combustion front is stabilized. In the case of nonuniform radial inlet flow velocity distribution, the ignition takes place in the radial cross-section with higher reaction mixture flow rate. Higher transient radial temperature gradients and lower axial temperature gradients exist in comparison with the case with the uniform inlet flow velocity distribution. After the stabilization of temperature pattern, we can observe only small differences in resulting temperature patterns, e.g., lower radial temperature gradients in the rear part of the reactor for uniform inlet velocity distribution, cf. Figs. 3 and 5. Differences in spatiotemporal temperature patterns also arise when the inlet temperature is close to ignition temperature and/or fast heating of the monolith from the ambient temperature to ignition temperature takes place. In this case, the effect of nonuniformity is particularly important (cf. Fig. 5).

The dynamics of reaction front motion strongly depends on inlet temperature, concentrations, flow rate conditions, and previous history of development of spatiotemporal patterns. The presented results illustrate the existence of two types of behavior: when the inlet temperature is sufficiently higher than the "light-off" temperature and the hot spot is formed at the monolith entrance, then the formed temperature hot spot becomes stationary and no travelling front has been observed. In the second case, when the inlet temperature is set only slightly higher than the "light-off" temperature, the hot spot is established at the rear part of the reactor and propagates towards the face of the monolith. It can be stabilized either in the central part of the reactor or close to the face of the monolith.

In the cases, shown in Fig. 5, the velocity of the propagation of the temperature front approximately was 2 mm/s, and the time necessary for the stabilization of the position of the hot spot was in the order of tens of seconds. When an order of magnitude lower flow rates were used [14], similar types of propagation of hot spots were observed, however, the velocities of propagation were an order of magnitude lower and the time for stabilization of profiles was accordingly longer.

3.2. Evolution of spatiotemporal temperature patterns in periodically operated monolith

Complex arrangements of monolithic reactors, including combinations of several monoliths, flow reversal and various heating and cooling schemas were proposed recently for use in automobile converters. One of the proposed arrangements makes use of two monolithic reactors with alternating flow of the reacting gases and cooling air into the monolith to set up proper axial temperature profile along the monolith for NO reduction catalysts operating in relatively narrow temperature window [5,6].

In the following, we present results of experiments performed in order to study the dynamic behavior of spatiotemporal temperature patterns in the monolithic reactor under periodic variation of inlet conditions. The detailed knowledge of the patterns can be used, for example, for the design of control algorithms of periodically operated monoliths. Both uniform and nonuniform inlet flow velocity distributions were used.

The experiments were carried out under an experimental protocol different from that for the above-described "light-off" experiments. At the start of the experiment, the reactor was operated under

Table 2
Inlet conditions, experiments with periodic inlet conditions variation, the half-period 44 s

figure*	Inlet temperature (°C)	Cooling temperature (°C)	Concentration of CO (vol.%)	Flow rate (l/min)	
				Reacting	Cooling
6	225	20	1	75	75
7	250	20	1	75	60
8	290	20	1	75	60

conditions where the reactions occurred with high conversion and the temperature profile has been stabilized. Then the periodic variation of the inlet stream conditions was started. It was realized as periodic switching between the reaction mixture (heated to higher than the "light-off" temperature, cf. Table 2) and the cooling air. Temperature pattern measurements were realized either by dynamic shifting of thermocouples within the monolith (dynamic measurements) or by repeated recording of temperatures at chosen different axial positions until the stationary state temperature profile has been reached (stationary measurements).

Temperature patterns obtained by dynamic measurements (shifting of thermocouples) are depicted in Fig. 6. The first row of patterns in Fig. 6 shows the course of temperatures after the start of periodic variations of conditions in the inlet stream. Temperatures were recorded for every 2 s at 12 different axial positions (hence one cycle of the spatiotemporal pattern was recorded within 22 s) and the inlet conditions were varied with the half-period of 44 s (the flow of both the reaction mixture and the cooling air lasted for 44 s).

At the time of the first switching, the thermocouples were placed 10 mm from the entrance to the monolith, cf. Fig. 6, the first snapshot. The next snapshot shows cooling of the monolithic structure after switching to cooling air. There is evident nonuniform temperature distribution corresponding to the nonuniform inlet flow distribution with maximum in the center. The situation after the switching to reacting gas corresponds to the third snapshot. Due to high surface temperature at the rear part of the reactor, the reaction takes place predominantly in this area (relatively high axial temperature gradients exist in the middle part of the reactor), cf. the third and fourth snapshots. The following snapshots depict stabilization of temperature profiles inside the reactor and the last two rows of snapshots document the periodicity of the established temperature pattern. The stabilization of periodic course of outlet CO_2 concentration and practically constant outlet temperature are depicted in the top part of Fig. 6. However, due to low inlet temperature, the overall CO conversion is low.

The dynamic measurement procedure offers general information about the development of spatiotemporal temperature patterns in the case of relatively slow development of temperatures inside the reactor or for long periods of variation of inlet parameters. To obtain more detailed information on the evolution of temperatures in the reactor, the repeated (continuous) measurements at constant positions along the reactor were used ("stationary measurement"). Temperature patterns obtained in this manner are depicted in Fig. 7. Higher inlet temperature than one used in Fig. 6 leads to far higher CO conversions.

Temperature patterns were measured under the following conditions:

- after the "light-off", the stationary temperature spatial pattern was established;
- the switching procedure (variation of inlet conditions) has been started and periodic switching of inlet conditions continued until the periodic spatiotemporal pattern has been established;
- the datalogging of temperatures at each axial position for 12 periods (i.e., 1056 s) started.

The first snapshot in Fig. 7 corresponds to the temperature pattern at the start of the flow of the hot reacting mixture (legend above the picture denotes time from the start of the period). Radially nonuniform flow velocity profile with maximum at the center has been again used. In the next snapshot, we can observe increasing temperatures in the front part of the monolith following the inflow of the hot reaction mixture and slightly increasing rear area temperatures

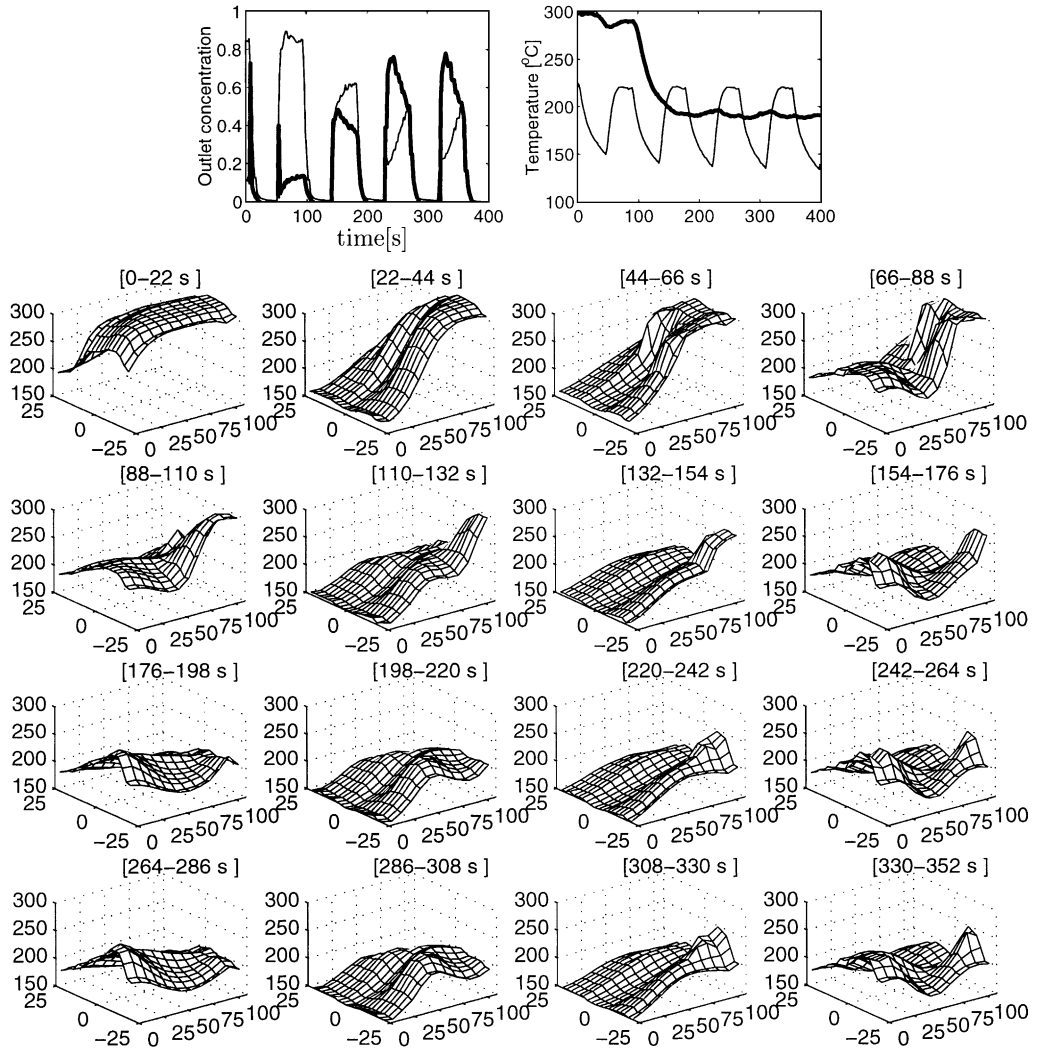

Fig. 6. (Bottom): Evolution of spatially 2D temperature patterns within the monolithic reactor, periodic variation of inlet conditions (alternating flow of reacting gas and cooling air), dynamic measurement, *nonuniform* inlet flow velocity distribution, *x*-axis axial (mm), *y*-axis radial (mm), *z*-axis temperature (°C); (top): course of outlet concentrations (volume averaged) in vol.% (CO — thick line, CO_2 — thin line), temperature-inlet (thin line) and outlet (thick line).

due to the heat of reaction (CO oxidation). The following snapshots show progressively increasing temperatures in the front part of the monolithic reactor where the rate of reaction is increasing. The propagation of the reaction front to the front part of the reactor is evident from the course of the outlet temperature, cf. Fig. 7 which slightly decreases with time even if the inlet temperature is high. This can also be seen from the temperature pattern in the second row of the snapshots. The axial temperature gradients are reduced and spread out. The reactor cooling process after the switching to the flow of the cooling gas is depicted in the following snapshots. The similarity of snapshots at 0 and 84 s confirms the periodicity (period 88 s) of the observed spatiotemporal temperature patterns, demonstrated also by the course of outlet CO_2 concentration and temperature (Fig. 7).

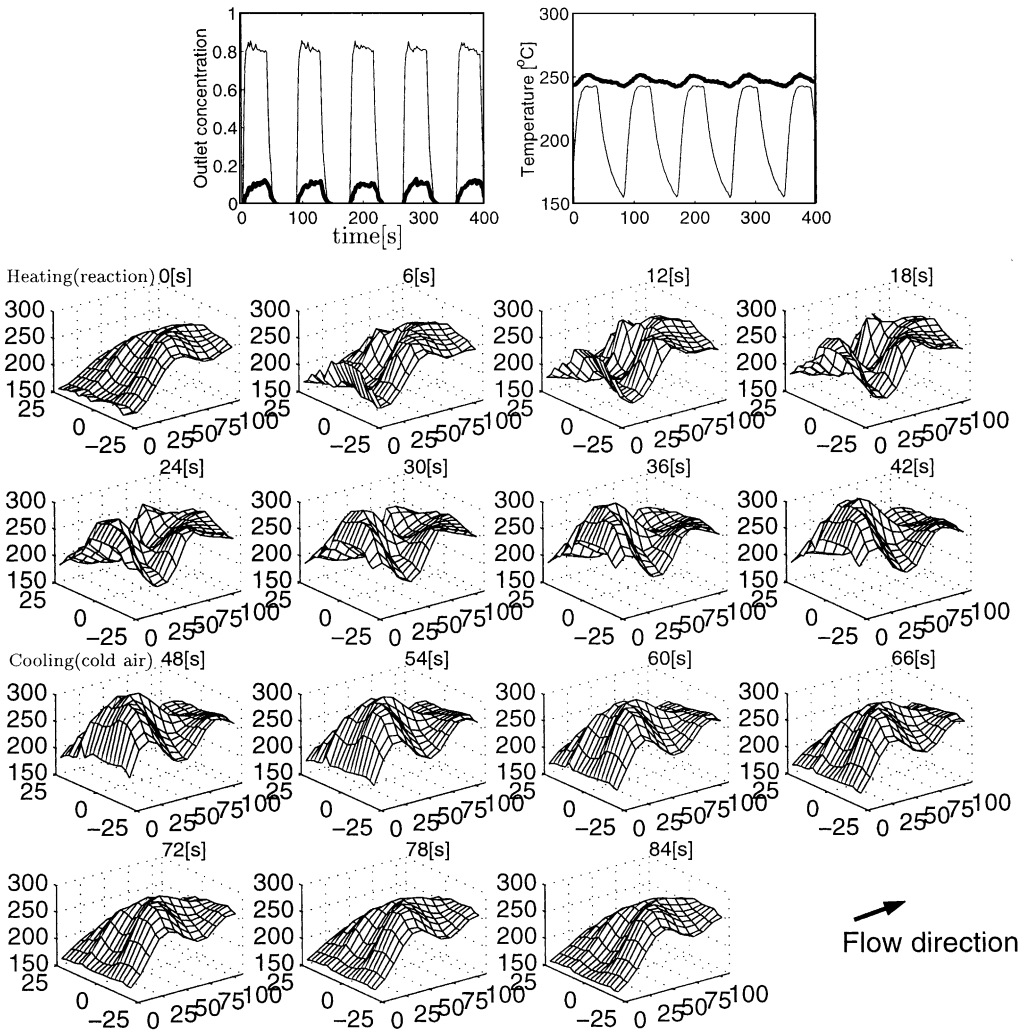

Fig. 7. Evolution of spatially 2D temperature patterns inside the monolithic reactor (bottom), periodic variation of inlet conditions (alternating flow of reacting gas and cooling air), reconstructed profiles — stationary periodic profiles, *nonuniform* inlet flow velocity distribution; *x*-axis axial (mm), *y*-axis radial (mm), *z*-axis temperature (°C); (top): course of outlet concentrations (volume averaged) in vol.% (CO — thick line, CO_2 — thin line), temperature-inlet (thin line) and outlet (thick line).

The evolution of temperature patterns for uniform inlet flow velocity distribution is depicted in Fig. 8. The experimental protocol was the same as in the case of the nonuniform inlet flow velocity distribution and the layout of the graphs also agrees. The figure depicts the situation where the reaction front at the start of the heating period is located in the middle part of the monolith. In the course of the heating (reaction) period, new reaction front is initiated in the front part of the reactor and in the cooling period, the front then propagates into the middle part of the reactor and the temperature decreases. Comparison of Figs. 7 and 8 illustrates how contrary to smooth, radially uniform spatial temperature profiles for radially uniform inlet flow velocity (e.g., measured in the laboratory, cf. Fig. 8), more complex radially nonuniform profiles are observed (cf. Fig. 7) for nonuniform inlet flow distribution typical in car mufflers. Comparison of

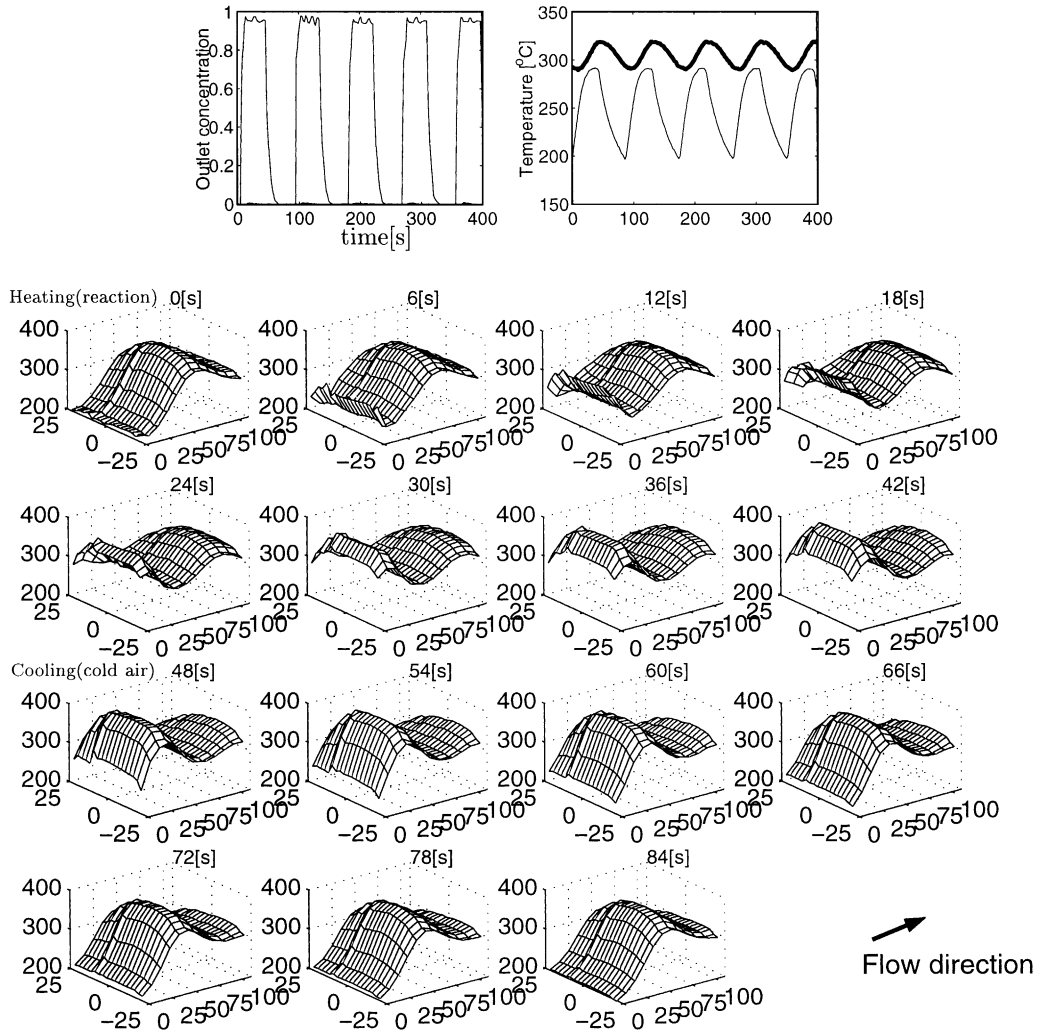

Fig. 8. Evolution of spatially 2D temperature patterns inside the monolithic reactor, periodic variation of inlet conditions (alternating flow of reacting gas and cooling air), reconstructed profiles — stationary periodic profiles, *uniform* inlet flow velocity distribution, *x*-axis axial (mm), *y*-axis radial (mm), *z*-axis temperature (°C); (top): course of outlet concentrations (volume averaged) in vol.% (CO — practically zero, CO_2 — thin line), temperature-inlet (thin line) and outlet (thick line).

spatiotemporal temperature patterns in both the cases confirms that the temperature within the monolith is kept in a relatively narrow range between times 18 and 42 s in the reacting period.

3.3. Selective catalytic reduction of NO_x under lean burn conditions

The results of experiments where reaction mixture (propene 1700 ppm and NO 550 ppm in air) flows through the reactor under constant inlet temperature agree with the earlier published experimental data [3]. The peak of conversion for NO_x reduction (40%) coincides with the ignition temperature of propene combustion. The inlet temperature corresponding to the peak point is characteristic for the used catalyst. Partial reduction of NO by propene is observed below this temperature, while in this temperature range, NO to NO_2 oxidation does not take place. For higher temperatures the NO oxida-

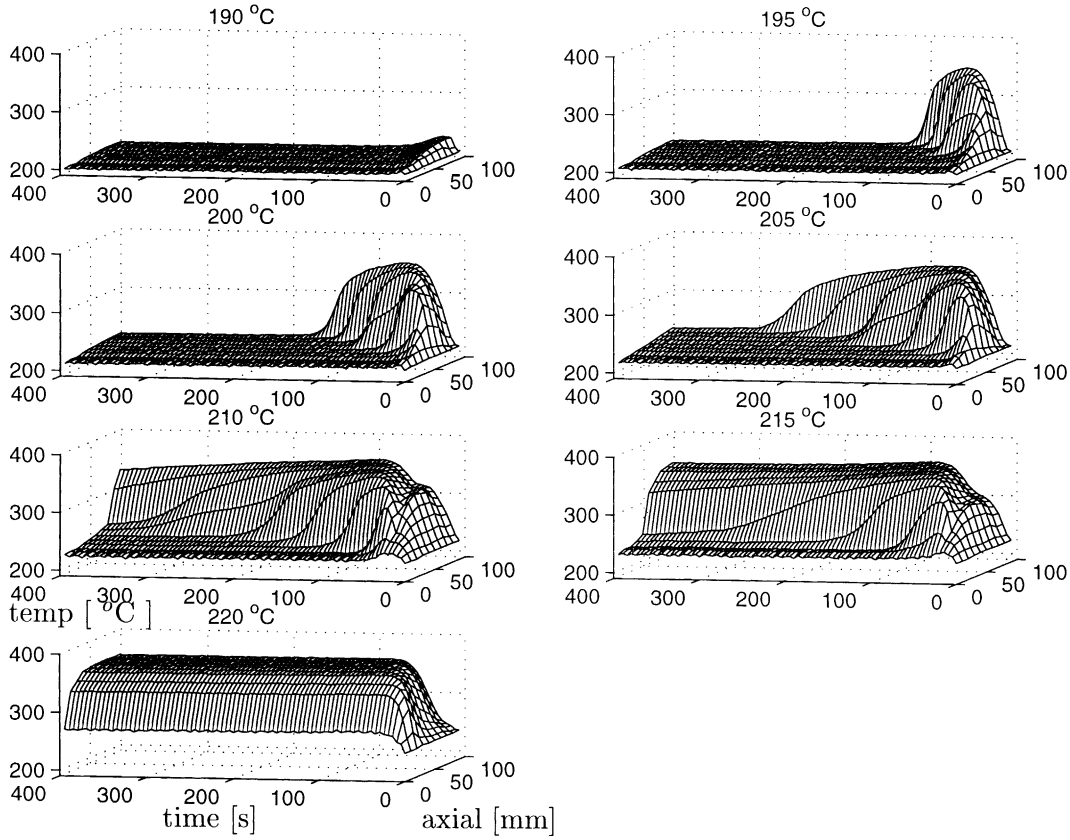

Fig. 9. The course of temperature profiles in ceramic monolithic reactor, "light-off" behavior for different inlet temperatures, mixture containing propene (1700 ppm) and NO (550 ppm) in air, legend denotes inlet temperature (°C), uniform inlet flow distribution.

tion starts and continues until maximum conversion is reached and total conversion for NO_x reduction decreases.

Simultaneous observation of outlet conversions and temperatures together with the recording of the evolution of spatiotemporal patterns can help to identify the effects of the individual variables. This is illustrated below for the case of NO inhibition of propene combustion. It has been observed in stationary experiments that for relatively narrow temperature window, an "inhibition" of propene oxidation by NO took place. In the temperature range 185–205°C, the ignition at first occurs, but then the extinction is observed. If NO is not present, the extinction in this temperature range does not occur. Time course of axial temperature profiles inside the monolith for this case is depicted in Fig. 9 for ceramic monolith. Reaction is ignited at the end of the reactor and the ignited reaction front propagates into the front part of the reactor. The inhibition prevents the propagation and thus causes the blow-out of the reaction front for lower inlet temperatures.

The effect of inhibition was confirmed by observations in the cases where NO was added after propene oxidation took place with maximal conversion. Fully ignited reactor becomes extinguished after the addition of NO in the range of inlet temperatures 190–210°C for ceramic monolith. The corresponding time courses of reactor temperatures are depicted in Fig. 10. The figure shows the behavior after NO addition into the reaction mixture at time 250 s. The maximum reactor temperature increases while the temperature in the front part of the reactor decreases even if the reaction has not been totally blown out. For the lowest

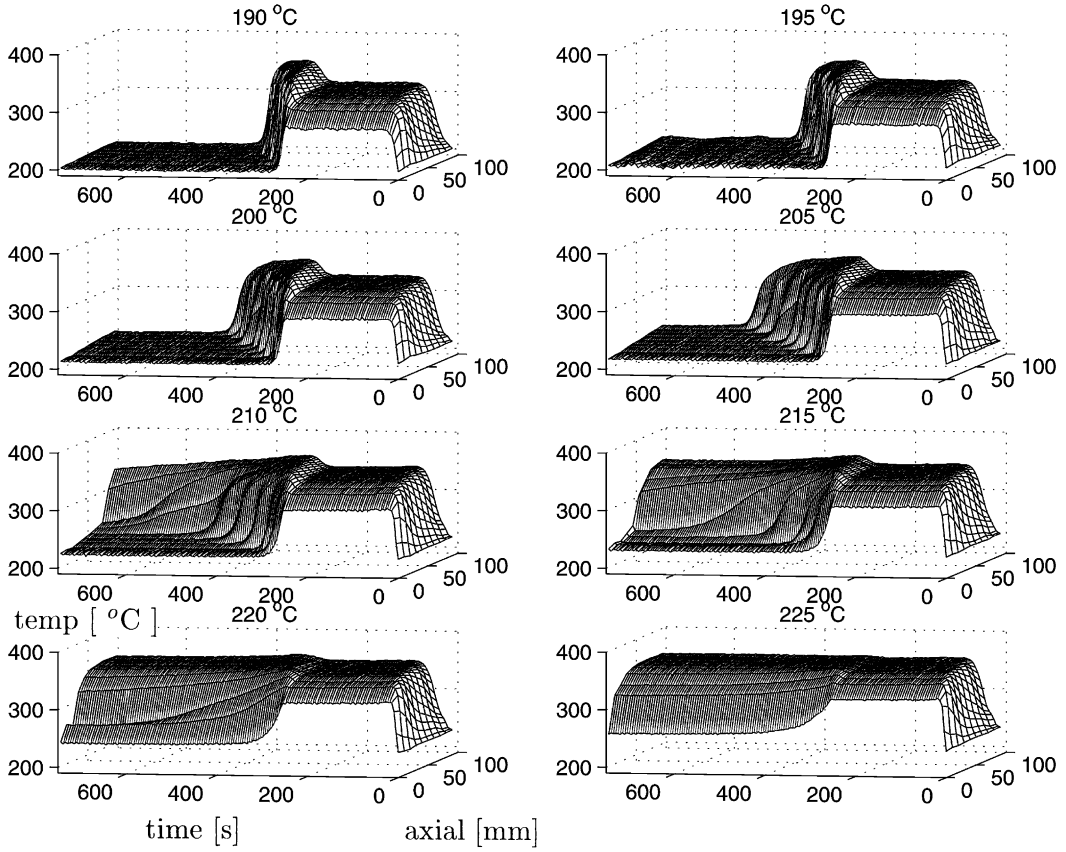

Fig. 10. Evolution of temperature profiles in ceramic monolithic reactor, "light-off" behavior for different inlet temperatures, mixture containing propene (1700 ppm) in air; addition of NO (550 ppm) into reaction mixture at 250 s, legend denotes inlet temperature (°C), uniform inlet flow distribution.

Table 3
Comparison of the stationary and non-stationary operations, mean outlet concentrations and conversions, ceramic monolith, inlet concentrations: 550 ppm NO, 1700 ppm propene

	Steady state operation		Non-stationary operation	
T_{in}	250°C	275°C	250°C	275°C
CO_2 (vol.%)	0.55	0.55	0.52	0.53
C_3H_6 conversion	0.97	0.97	0.91	0.94
NO (ppm)	11	208	152	146
NO_x (ppm)	441	475	291	344
NO_x Conversion	0.2	0.13	0.47	0.37
Cooling air flow rate (l/min)		–	75	100
Half-period (s)	–	–	20	30

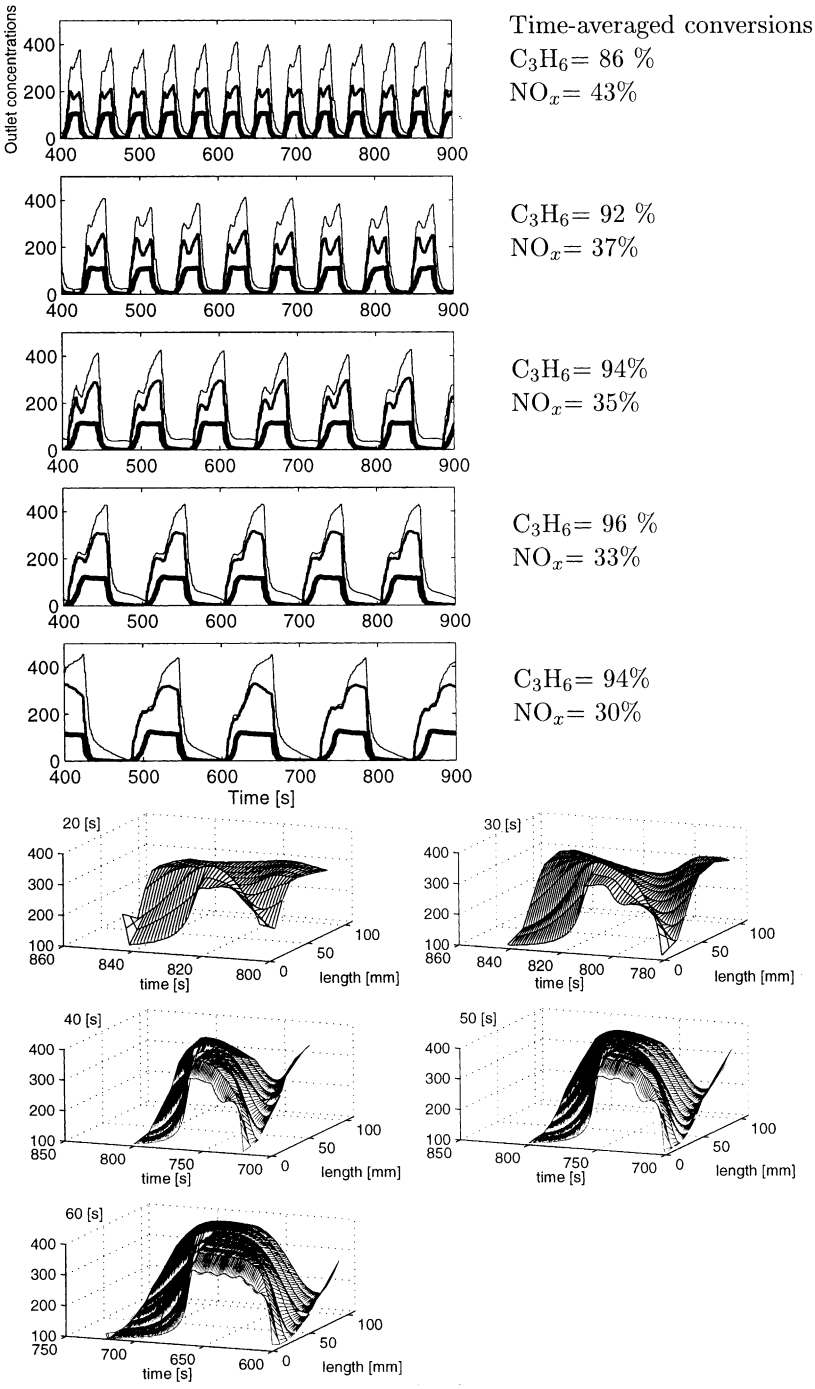

Fig. 11. Course of outlet concentrations (top), NO_x (ppm) — thin curve, NO (ppm) — medium thickness curve, $CO_2 \times 200$ [vol.%] converted propene — thick curve, and temperature patterns in the metallic monolithic reactor (bottom) for five values of switching half-period. Cooling flow rate 75 l/min, $T_{in} = 275^{\circ}C$.

reported inlet temperatures (190–205°C), the reaction front starts to move after the addition of NO relatively fast through the reactor (velocity between 0.6 and 2.5 mm/s) from the face of the monolith to the rear part of the monolith where it ceases to exist. For higher temperatures, the reaction front is not so sharp. The behavior after propene addition into the reaction mixture containing only NO and air is very similar to the case of the complete reaction mixture, i.e., propagation of the ignition front followed by the extinction in the defined range of inlet temperatures, cf. Fig. 9. However the NO/NO_x desorption peaks were observed after the flow of propene into the reactor was started.

3.4. Periodic variation of inlet stream composition

Switching between two identical thermally coupled reactors has been followed earlier in the computational study, cf. [5,6]. It has been predicted that the establishment of proper temperature profile in the case of relatively narrow temperature window for NO_x reduction can lead to improved integral NO_x conversion, cf. Fig. 12. This is also supported by experimental results on periodic switching at the inlet between the reacting and cooling gas discussed above. In the experimental study, a modified system consisting of a periodically operated single reactor was used. Hence the heat exchange between two reactors was not present in this case. It was considered that the behavior of the second reactor will be the same after a stabilized periodic regime is achieved. The monoliths with channel density 400 CPI and a catalytic layer consisting of Al_2O_3 and active metal Pt were used. The flow rate conditions and the inlet temperature used in the experiments correspond to typical ranges for the treatment of exhaust from diesel engines. Flow rate of the inlet gas was set to SV = 30 000 h^{-1} (125 l/min STP) and the inlet temperature has been varied in the range from 250 to 350°C. The reaction mixture was prepared from air (high oxygen excess — lean burn conditions) and reacting species (propene and NO only). The experiments were carried out for five values of the switching half-period (from 20 to 60 s with 10 s step) and five flow rates (50, 75, 100, 125 and 150 l/min (STP)). The relevant range of the half-periods was determined experimentally considering also the response time of the available analytical equipment.

The course of experiments was as follows. The reactor temperature was set by passing hot air. Then the reaction mixture (propene 1700 ppm, NO 550 ppm) was injected into the reactor and at the same time scanning of temperatures (inlet, outlet and within the reactor) and outlet concentrations was started. Switching between the reaction half-period, where the reaction mixture passes through the reactor and the cooling half-period, where the ambient air flows through the reactor occurs until the outlet concentrations and temperature profiles were stabilized. Usually 900 s of periodic operation was sufficient to reach the stationary values.

Example of the evolution of outlet concentrations in time and axial temperature patterns (temperatures in the center of the monolith were recorded, cf. Fig. 2) in the course of one period for five values of the switching half-period are shown in Fig. 11. The first row (top

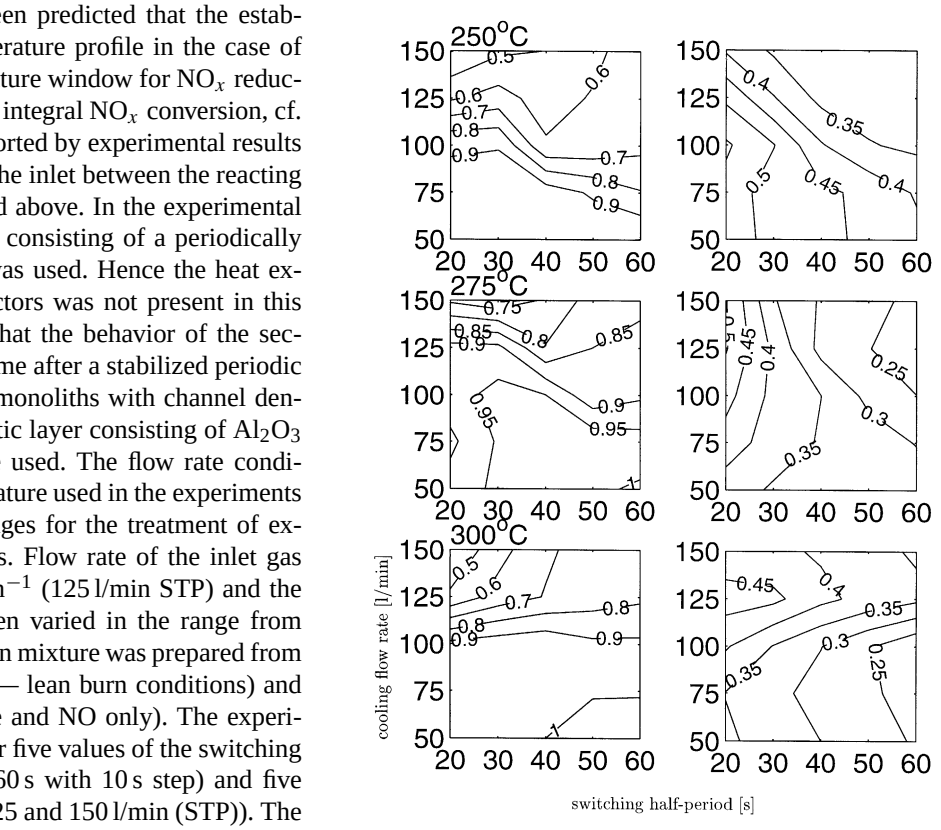

Fig. 12. Ceramic monolith, mean outlet conversions of propene (left) and NO_x (right) for different inlet temperatures in dependence on switching half-period and cooling flow rate.

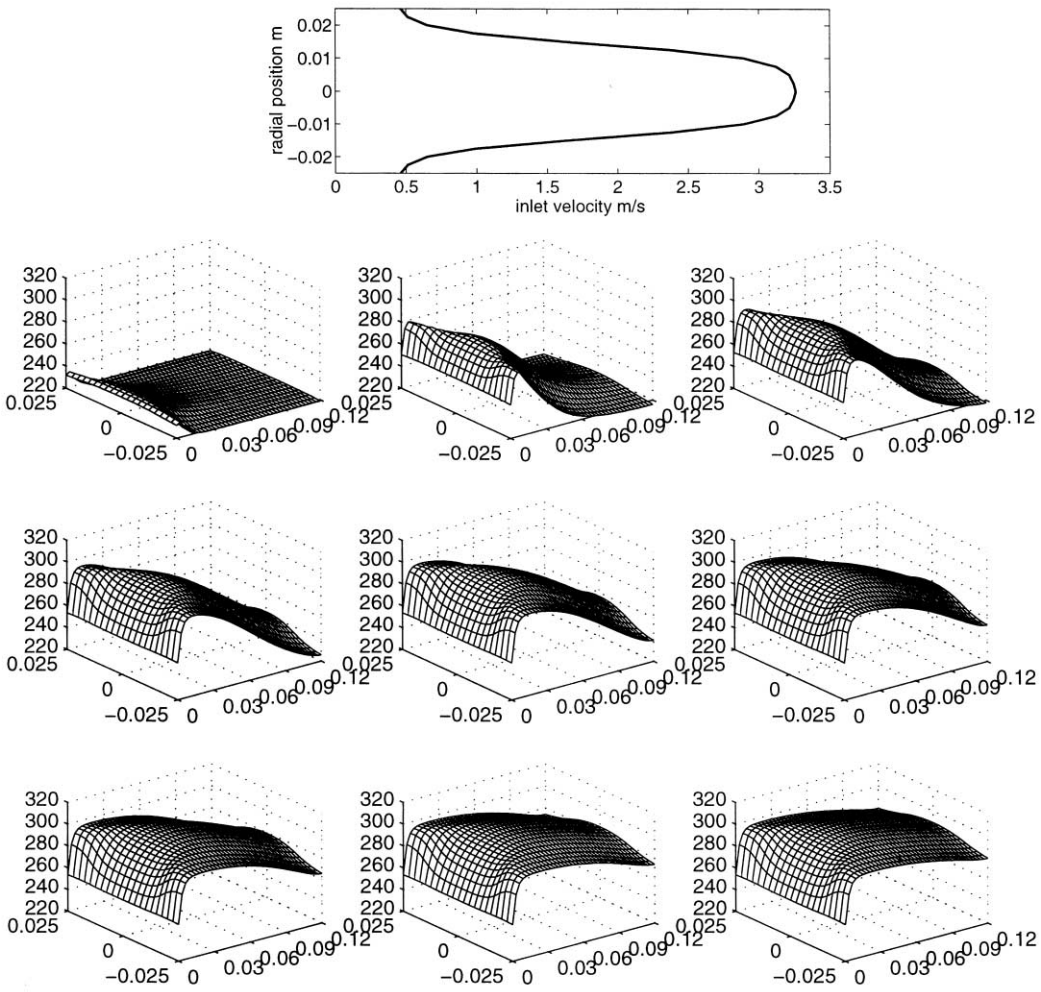

Fig. 13. Top: Radially nonuniform (parabolic-like) inlet flow velocity distribution into monolith used in simulations for space velocity $30\,000\,h^{-1}$, bottom: Course of temperature patterns in monolithic reactor, *nonuniform* inlet flow distribution, $V_{in} = 75 l/min$, $T_{in} = 220°C$; computations based on two-phase quasihomogeneous model, *x*-axis axial (m), *y*-axis radial (m), *z*-axis temperature (°C).

picture) corresponds to the situation where the switching time was set to the shortest value (20 s) and the cooling process is not so intensive. Hence, the reactor temperature is relatively stationary at the rear part of the monolithic reactor, cf. spatiotemporal temperature profiles at the bottom of Fig. 11. Therefore the ignition and the peak of the NO_x outlet concentration are reached fast. For longer switching half-periods, the "light-off" process has a short time-lag and a decrease of NO_x concentration occurs first. Then the propene combustion is ignited and the NO_x concentration increases again. Time averaged values of outlet conversions show that the highest conversion is reached for the shortest switching period.

The summarized representation of experimental results — mean outlet conversions — in dependence on inlet temperatures, switching half-period and cooling intensity (flow rate) are depicted in Fig. 12. Generally, the lowest time-averaged outlet concentrations of NO_x were obtained in the region of short switching half-periods. NO conversions were higher than in the stationary operation, c.f. also Table 3.

4. Comparison of experiments and simulations

Modular software for simulations of monolithic catalytic reactors and adsorbers has been developed [15]. Only qualitative and in some cases semiquantitative agreement can be expected between spatiotemporal temperature patterns observed in experiments and patterns computed on the basis of mathematical models, particularly in spatially 2D cases. This follows from the missing knowledge of the actual spatial distribution of activity of the catalyst in the monolith and empirical character of complex kinetic relations, particularly in the case of selective catalytic reduction of NO [16–19]. Example of evolution of temperature in the monolith in the case of nonuniform radial inlet distribution of flow velocities into monolith, cf. top of Fig. 13, where only CO oxidation takes place on a catalyst Pt/Al_2O_3 (cf. Fig. 4), based on a two-phase quasi-homogeneous model, cf. also [20], is shown in Fig. 13. We can observe that similarly as in the case of experimental profiles shown in Fig. 4, the "light-off" starts in the front part of the reactor with the highest temperature in the central part of the monolith, where the flow rate is highest, and then temperature rises in the entire reactor.

5. Conclusions

Experimentally determined temperature and concentration spatiotemporal patterns confirm that even if final stationary spatial temperature patterns mostly correspond to the situation where the "light-off" occurs at a small distance from the inlet to the monolith, actual non-stationary situation can be different. Non-stationary experiments illustrate that the ignition can start at the end or in the central parts of the monolith and temperature maximum then propagates to the front part of the monolith. Nonuniform inlet flow velocity distribution with maximum in the center causes ignition to occur in the central part of the monolith, and then the developing radial temperature profiles are also nonuniform.

Non-stationary experiments with periodic alternation between the flows of reacting gases and cooling air at the inlet illustrate that periodically varying temperature pattern in the monolith can be kept within values, approximating, e.g., temperature window for high NO conversion.

The possibility of reaching higher conversion of NO_x in non-stationary periodic operation than in the standard stationary process has been also experimentally demonstrated. The presented measured spatiotemporal patterns can be used as an inspiration for detailed mathematical modeling, particularly in the case of NO_x selective catalytic reduction.

Acknowledgements

This work was supported by Czech Ministry of Education (Project MSM 223400007).

References

[1] A. Cybulski, J.A. Moulijn, Structured Catalyst and Reactors, Marcel Dekker, New York, 1998.
[2] G.P. Ansell, P.S. Bennet, J.P. Cox, J.C. Frost, P.G. Gray, A.-M. Jones, R.R. Rajaram, A.P. Walker, M. Litorell, G. Smelde, Appl. Catal. B 10 (1996) 183.
[3] R. Burch, J.A. Sullivan, T.C. Watling, Catal. Today 42 (1998) 13.
[4] Y. Ikeda, K. Sobue, S. Tsuji, S. Matsumoto, SAE Paper 1999-01-1279 (1999).
[5] J. Jirát, F. Štěpánek, M. Kubíček, M. Marek, Chem. Eng. Sci. 54 (1999) 2609.
[6] J. Jirát, F. Štěpánek, M. Kubíček, M. Marek, Chem. Eng. Technol. 24 (2001) 35.
[7] W. Taylor, SAE Paper 1999-01-0454 (1999).
[8] S. Siemund, J.P. Leclerc, D. Schweich, M. Prongent, F. Castagna, Chem. Eng. Sci. 51 (1996) 3709.
[9] P. Pinkas, D. Šnita, M. Kubíček, M. Marek, Chem. Eng. Sci. 49 (1994) 5347.
[10] R. Jahn, D. Šnita, M. Kubíček, M. Marek, Catal. Today 38 (1997) 39.
[11] J. Howitt, T. Sekella, SAE Paper 740244 (1974).
[12] D. Wendland, W. Matthes, SAE Paper 861554 (1986).
[13] D. Chen, S. Oh, E. Bisset, D. Ostrom, SAE Paper 880282 (1988).
[14] D. Šnita, R. Jahn, M. Kubíček, M. Marek, Combustion in multichannel monolithic reactors: modelling and experiments, AIDIC Conference Series, Vol. 2, Selected Papers of the First European Congress on Chemical Engineering, Milano, 1997, p. 95.
[15] J. Jirát, M. Kubíček, M. Marek, Chem. Eng. Sci. 56 (2001) 1597.
[16] G. Koltsakis, P. Konstantinidis, A. Stametelos, Appl. Catal. 12 (B) (1997) 161.
[17] S. Jeong, W. Kim, SAE Paper 980881 (1998).
[18] E. Massing, J.F. Brilhac, A. Brillard, P. Gilot, G. Prado, Chem. Eng. Sci. 55 (2000) 1707.
[19] H. Oh, J. Cavendish, Ind. Eng. Chem. Proc. Res. Dev. 12 (1982) 28.
[20] K. Zygourakis, Chem. Eng. Sci. 44 (1989) 2075.